Laser Raman spectroscopy (LRS) and time differential perturbed angular correlation (TDPAC) study of surface species on Mo/SiO_2 and $Mo,Na/SiO_2$. Their role in the partial oxidation of methane

A.J. Marchi, E.J. Lede [a], F.G. Requejo [a], M. Rentería [a], S. Irusta, E.A. Lombardo and E.E. Miró

Instituto de Investigaciones en Catálisis y Petroquímica – INCAPE (FIQ, UNL, CONICET), Santiago del Estero 2829, 3000 Santa Fe, Argentina

[a] *Departamento de Física, Fac. de Ciencias Exactas, UNLP and TENAES (CONICET), Argentina*

Received 25 April 1997; accepted 14 August 1997

Silica-supported molybdenum (1.6 and 5.0 wt%) and molybdenum (5 wt%)–sodium (0.4 wt%) catalysts have been characterized by laser Raman spectroscopy (LRS), time differential perturbed angular correlation (TDPAC), temperature-programmed reduction (TPR) and X-ray photoelectron spectroscopy (XPS). The presence of different molybdenum species was correlated with activity and selectivity to formaldehyde during the methane partial oxidation reaction. The main species identified on the Mo(5.0 wt%) / SiO_2 surface were MoO_3 and monomeric species with a single Mo=O terminal bond. The pre-impregnation of the silica support with sodium strongly diminishes the Mo=O concentration due to the formation of $Na_2Mo_2O_7$ species and tetrahedral monomers with a high degree of symmetry. As a result of these modifications, both methane conversion and formaldehyde formation are strongly inhibited. The combination of LRS and TDPAC techniques resulted in a powerful tool for the identification and quantification of the molybdenum species present on the surface of a silica support.

Keywords: molybdenum surface species, silica-supported catalysts, methane partial oxidation, sodium poison, Mo=O sites

1. Introduction

The conversion of methane to higher valued products has attracted the attention of many research groups in the last decade, not only for its industrial applications but also for its academic value. Among the catalysts investigated, Mo/SiO_2 and V/SiO_2 have received special attention in the last few years for their ability to oxidize methane to formaldehyde [1,2]. Several studies have been published about the link between active sites and their role in the reaction mechanism. The negative effect of sodium upon activity and selectivity has been first reported by Spencer and co-workers [3,4]. In this vein, Bañares et al. [5,6] also produced interesting results, especially by their study of the effect of Na, K and Cs upon the catalytic behavior of Mo/SiO_2. They suggested that the negative effect of sodium on Mo/SiO_2 catalysts is due to a strong nucleation effect of sodium which forms new alkali–molybdate clusters. Koranne et al. [7] using transient methods suggested that a redox mechanism takes place on V/SiO_2, while Kartheuser and Hodnett [8] correlated the dispersion of vanadium oxide on silica with the selectivity to formaldehyde. We have previously reported [9,10] that the formaldehyde yield correlates with the vanadyl (V=O) concentration on the catalyst surface. The addition of sodium promotes the formation of non-distorted orthovanadate-like tetrahedra with very low or none vanadyl character. Thus the methane molecule cannot be activated through hydrogen abstraction, thus explaining the low activity of the sodium-modified catalyst. Furthermore, this species can decompose the formaldehyde to carbon monoxide, which explains the low selectivity observed.

For the Mo/SiO_2 catalyst, the role played by the different molybdenum-containing species in the oxidation of methane to formaldehyde has been a matter of controversial interpretations. Bañares et al. [5] proposed that highly dispersed monomeric species of molybdenum oxide are the active sites for the formaldehyde formation, while Suzuki et al. [11] concluded that well-dispersed molybdenum oxide clusters on SiO_2 support are the active species. On the other hand, Smith and Ozkan [12] proposed that the Mo=O sites present in the MoO_3 crystals are catalytically active while Mo–O–Mo accelerates the deep oxidation of methane.

Wachs and co-workers [13,14] thoroughly characterized MoO_3 supported on different oxides. They concluded that the surface molybdenum oxide structures, under ambient conditions, are dependent on the net surface pH at PZSC (point of zero surface charge). For low molybdenum loading on silica support, and under dry conditions, only monomeric species were detected.

In this work, we report results on the characterization of surface species present in Mo/SiO_2 and $Mo,Na/SiO_2$

using laser Raman spectroscopy (LRS), X-ray photoelectron spectroscopy (XPS) and the time differential perturbed angular correlation technique (TDPAC). The Mo/SiO_2 catalyst was poisoned with sodium with the aim of gaining further insight in the structure of the active sites in the oxidation of methane to formaldehyde similarly to what has been previously done with V/SiO_2 [9,10].

2. Experimental

A commercial non-porous silica Cabot M5 Aerosil-particle size 5–30 nm, BET area 200 $m^2\,g^{-1}$ and composition $SiO_2 > 99.8\%$, $Al < 5$ ppm, $Fe < 2$ ppm, and $Na < 0.5$ ppm was used as a carrier. This was impregnated during 12 h with aqueous solutions in appropriate amounts so as to yield solids with 1.6 and 5 wt% molybdenum. The impregnated solids were dried at 393 K and calcined 2 h at 473 K and 12 h at 873 K. The amount of metal loading is defined as the ratio of the weight of metal divided by the total weight of the catalyst on a percent basis. We have used a higher content of Mo than Bañares et al. [5] in order to favor the formation of small crystals of the MoO_3 dispersed on the surface of SiO_2 that increases the activity of these catalysts [11]. A catalyst containing sodium as well was prepared by washing the silica support with 0.01 N sodium hydroxide, drying it prior to the molybdenum impregnation. This molybdenum–sodium–silica catalyst, which contains 5 wt% of molybdenum and 0.4 wt% of sodium, is denoted in the text as $Mo(5\%),Na/SiO_2$. The metal salts used for the impregnations were Merck pro-analysis ammonium heptamolybdate and sodium hydroxide.

The BET area of both catalysts was measured after calcination but prior to reaction using a Quantachrome Nova 2000 sorptometer. The XPS spectra were obtained at room temperature with an ESCA 750 computer-driven, Shimadzu instrument, using Mg Kα radiation. The Mo/Si, Na/Si, and O/Si atomic ratios were calculated using the area under the Si 2p, Mo $d_{5/2}$, Na 1s and O 1s peaks, the Scotfield photoionization cross-sections, the mean free paths of the electrons and the instrument function given by the ESCA manufacturer. The binding energies (BE) were always referred to C 1s at 284.6 eV.

Temperature-programmed reduction experiments were carried out using 0.08 g of sample which was pretreated in situ at 873 K during 2 h in dry oxygen. Following the treatment, the samples were cooled at room temperature and the gas switched to 5% H_2 in argon mixture. The gas flow was 25 cm^3/min and the temperature was raised at 10 K/min to 1073 K.

The LRS (laser Raman spectroscopy) was performed using a JASCO TRS-600SZ-P single monochromator spectrophotometer equipped with a CCD (charge-coupled device) with the detector cooled to about -120°C with liquid N_2. The excitation source, used to obtain the spectra, was the 514.5 nm line of a Spectra 9000 Photometrics Ar ion laser. The laser power, measured at the samples, was set at 30–40 mW. All the spectra were recorded with the samples under ambient conditions.

The surface structure of Mo/SiO_2 was studied by the electric field gradient (EFG) at the Mo-site employing the TDPAC technique. This technique, through the measurement of the local electric field gradients (EFG) at the radioactive probe site, can give information about the characteristics (coordination, symmetry, distortions, etc.) of the different environments of the probes, their concentration and modifications related to in situ conditions. Compounds containing molybdenum have the advantage that after neutron irradiation the TDPAC probe ^{99}Mo is formed from natural ^{98}Mo. Thus, the extracted information is reliable since the TDPAC probe does not introduce an impurity. A brief and clear description of this technique and of the typical equipment set up has been published by Butz et al. [15].

An experimental arrangement of four CsF coplanar detectors at 90° for a fast–slow coincidence system was used. The equipment resolution time was 0.8 ns and the calibration 0.29 ns/channel. For the TDPAC measurements the γ–γ cascade 739–181 keV of ^{99}Mo was employed, the anisotropy of which is approximately 10%. The coincidence spectra were combined so as to obtain the asymmetry ratio $R(t)$ [16]. The isotope probe employed, ^{99}Mo, was produced by neutron irradiation of the samples in the RA-3 reactor of ''Comisión Nacional de Energía Atómica (CNEA)'', Argentina.

Steady-state kinetic experiments were performed using a single-pass flow reactor made of fused silica with an inside diameter of 1.8 cm and a heated length of 15 cm. In order to minimize formaldehyde oxidation in the gas phase, the diameter of the gas outlet tube was diminished to 0.1 cm immediately after the reaction zone. The reactor was loaded with 0.2 g of catalyst, and the total flow rate (methane plus oxygen) was 17 cm^3/min, with a CH_4/O_2 ratio of 9. Typically, methane conversions were measured between 793 and 973 K. Matheson Specialty Gases with the following purities were used: CH_4 (99.99%), O_2 (99.96%) and He (99.995%). Analyses of the feed and reactor effluent streams were performed by gas chromatography using a thermal conductivity detector. A Porapak T column was used to separate formaldehyde, carbon dioxide and water, and a molecular sieve 5A column for methane, oxygen and carbon monoxide.

3. Results and discussion

3.1. XPS and TPR characterization

Table 1 shows the BET surface areas and the Mo/Si surface ratios obtained by XPS for the $Mo(1.6\%)/SiO_2$,

Table 1
Surface area and composition of Mo/SiO_2 and $Mo,Na/SiO_2$ catalysts

Catalyst	Surface area [a] (m^2/g)	Mo/Si [b]	Mo (wt%)	Na (wt%)
$Mo(1.6)/SiO_2$	191	0.006	1.6	–
$Mo(5.0)/SiO_2$	178	0.02	5.0	–
$Mo(5.0),Na/SiO_2$	70	0.014	5.0	0.4

[a] BET method.
[b] Atomic ratios calculated using the area under the Si 2p and Mo $d_{5/2}$ peaks, the Scotfield photoionization cross-sections, the mean free path of the electrons and the instrument function given by the ESCA manufacturer.

$Mo(5\%)/SiO_2$, and $Mo(5\%),Na/SiO_2$ catalysts. The solid containing 1.6% Mo is similar to the one studied by Bañares et al. [5]. According to these authors, this calcined solid only has Mo monomers highly dispersed on the surface. Higher metal loadings lead to the formation of MoO_3. As shown in table 1, the increase in the amount of Mo from 1.6 to 5% only produces a slight decrease on the BET surface. However, the modification of the support with 0.4 wt% Na produces a decrease of ca. 60%. The XPS results show that the Mo/Si ratio increases from 0.006 to 0.02 with the increase of Mo loading while the addition of Na decreases this ratio by 30%. This is the opposite effect to what is observed for V/SiO_2 catalysts, in which the addition of Na produces a significant increase in the dispersion of vanadium [10].

Figure 1 shows TPR results for the $Mo(5\%)/SiO_2$ and $Mo(5\%),Na/SiO_2$ catalysts. The hydrogen consumption estimated using the area under the curves was similar for both solids. The main difference lies in the presence of a low temperature peak in the case of the Na-containing solid, this indicating either a higher dispersion of Mo, or else the presence of more easily reducible species. A higher dispersion of Mo is not coherent with the XPS results (table 1). Accordingly, the second hypothesis seems to be more adequate.

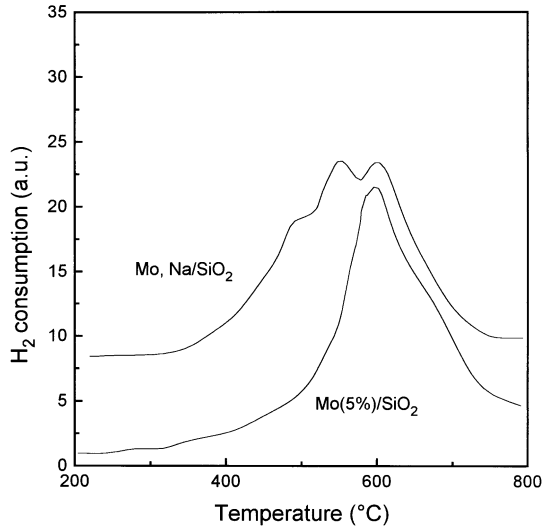

Figure 1. The effect of sodium on Mo/SiO_2 thermograms. TPR conditions: see experimental.

3.2. Raman characterization of $Mo(5\%)/SiO_2$ and $Mo(5\%),Na/SiO_2$

The most representative microscopic laser Raman spectra of Mo/SiO_2 and $Mo,Na/SiO_2$ samples, in the range of 700–1100 cm^{-1} are shown in figure 2. The assignment of the observed peaks is summarized in table 2.

In the case of the $Mo(5\%)/SiO_2$ sample, two intense peaks at 995 and 820 cm^{-1} and a broad, weak band between 960 and 980 cm^{-1} were observed (figure 2a). Instead, in the case of the $Mo(1.6\%)/SiO_2$ sample, the band at 820 cm^{-1} was practically not detected at the different regions examined in the sample (figure 2b). The peaks at 995 and 820 cm^{-1} are characteristic of crystalline MoO_3 and correspond to the stretching modes of the Mo=O terminal bonds and the Mo–O–Mo bridge bonds, respectively [17,18]. The spectrum obtained for the $Mo(5\%)/SiO_2$ sample would indicate that the MoO_3

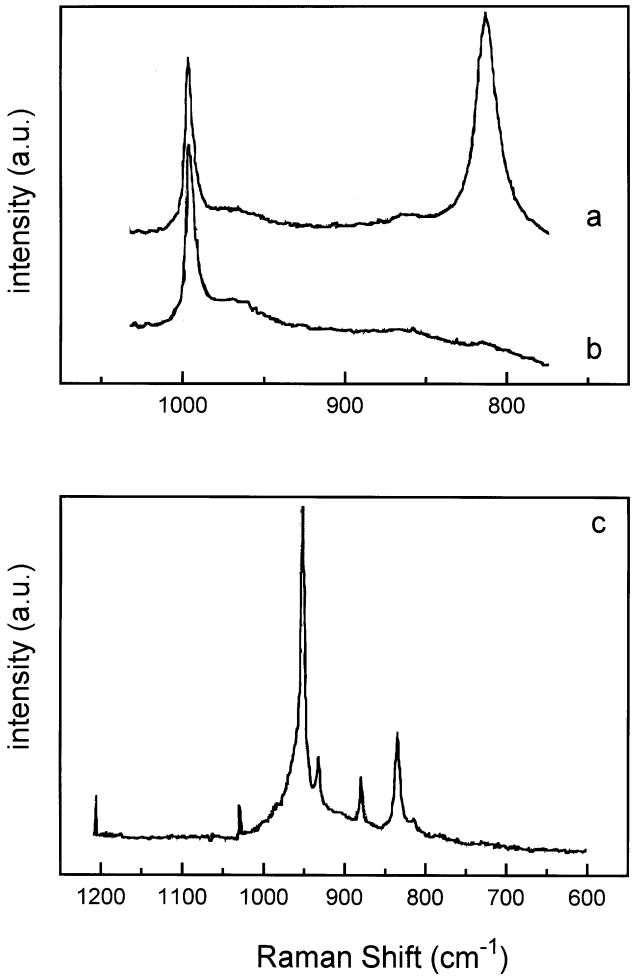

Figure 2. Laser Raman spectra. (a) $Mo(5\%)/SiO_2$, (b) $Mo(1.6\%)/SiO_2$, (c) $Mo(5\%),Na/SiO_2$.

Table 2
Band assigments in laser Raman spectra of Mo/SiO_2 and $Mo,Na/SiO_2$ catalysts

Identified species	Characteristic band (cm^{-1})	Catalyst		
		$Mo(1.6\%)/SiO_2$	$Mo(5\%)/SiO_2$	$Mo(5\%),Na/SiO_2$
octahedral monomer [a]	995	strong	strong	–
polymolybdate [b]	980–960	broad weak band	broad weak band	–
crystalline MoO_3 [c]	995	–	strong	–
	820	–	strong	–
	665	–	weak	–
crystalline $Na_2Mo_2O_7$-like species [d]	955	–	–	strong
	926	–	–	weak
	879	–	–	weak
	838	–	–	medium

[a] Refs. [11,17].
[b] Ref. [11].
[c] Refs. [15,16].
[d] Refs. [3,11,20].

is the main species formed on the surface of the support. The peak observed at 820 cm^{-1} was always considerably broad, indicating that the crystals of MoO_3 are small and disorderly structured. On the other hand, the I_{995}/I_{820} relative intensity of the LRS microscopic spectra of the $Mo(5\%)/SiO_2$ sample was in every case higher than that determined for a MoO_3 sample. Besides, in some cases LRS microscopic spectra similar to those of the $Mo(1.6\%)/SiO_2$ sample were obtained when different areas of the sample were focused with the laser beam (figure 2b). These results are in agreement with the presence of a second species over the surface of the support. The absence of peaks at 820 and 665 cm^{-1} indicates that these species do not have bridge bonds Mo–O–Mo. Therefore, they would be Mo monomers directly linked to the surface of the support [13,19]. The presence of a single band at 995 cm^{-1} would indicate that this monomeric species has only one Mo=O terminal bond, since species with two Mo=O terminal bonds would yield at least two bands in the stretching region [20]. The weak, broad band observed between 960 and 980 cm^{-1} is attributed to the stretching mode of Mo=O terminal bonds of polymolybdate-like species [13].

These results lead us to conclude that at least three types of species are present in the Mo/SiO_2 catalysts: (a) monomeric species with a single Mo=O terminal bond which would be the main species at low molybdenum loadings; (b) MoO_3 crystallites which would be the main species at high molybdenum contents; (c) polymolybdate-type species. The molybdate character of these species is important as suggested by the application of the frequency–length–strength (FLS) approximation [21]. From the peak at 995 cm^{-1} it was established that the Mo=O terminal bonds have a bond length of 1.687 Å and a bond order of approximately 1.92 u.v., both in the case of MoO_3 and in that of the monomeric species. In the case of the Mo–O–Mo bridge bonds, the lengths of the Mo–O bonds are 1.781 Å, obtained for 820 cm^{-1}, and 1.882 Å, considering the peak at 665 cm^{-1}.

The laser Raman microscopic spectra of the $Mo,Na/SiO_2$ sample present four well-defined peaks at 955, 926, 879 and 838 cm^{-1} overlapping a halo presenting a maximum at approximately 950 cm^{-1} (figure 2c). The sharp peaks at 955, 926, 879 and 838 cm^{-1} may be assigned to the presence of crystalline species of general formula $A_2Mo_2O_7$, where A is an alkaline metal as sodium or potassium [5,13,22]. The peaks at 955 and 926 cm^{-1} are normally assigned to the symmetrical stretch mode of Mo–O, while the bands at 879 and 838 cm^{-1} are assigned to the asymmetrical stretch mode of the Mo–O–Mo bridge bonds [13]. The formation of these species would result from the interaction of NaOH with the molybdenum precursor on the silica surface [5,13].

Williams et al. [13] found that on Mo/SiO_2 doped with 2% Na, the main species formed is Na_2MoO_4. However, when the Na loading was reduced from 2 to 0.5%, the presence of $Na_2Mo_2O_7$ was detected. Bañares et al. [5] found for low molybdenum contents that $Na_2Mo_2O_7$ was the main species formed on silica doped with sodium. These results are in agreement with ours. The doping of the silica surface with sodium leads to the formation of species with low molybdic character in which molybdenum has both tetrahedral and octahedral coordination, as in the case of $Na_2Mo_2O_7$.

To explain the formation of different species on both SiO_2 and SiO_2 doped with sodium, the pH change at the PZSC should be taken into account. The pH at PZSC for silica is approximately 4. The more stable molybdenum compounds in acid aqueous solution are those with octahedral coordination, i.e., $Mo_7O_{24}^{6-}$ and $Mo_8O_{26}^{4-}$. By applying this analogy, the three species detected by LRS in Mo/SiO_2 would have such structures that molybdenum would be occupying octahedral holes. This is true in the case of MoO_3 and polymolybdates formed on the

non-doped silica surface. Consequently, it could be expected that the third species detected, the monomer, also has an octahedral structure. In addition, this would be in agreement with the fact that no monoxo species in which molybdenum is in tetrahedral coordination are known so far [18]. When the silica surface is doped with 0.4% of sodium, the PZSC rises to higher pH [9]. It is known that for the case of supports with pH at PSZC of the order of 8 or higher, as in the case of Al_2O_3, the more stable structures are those in which molybdenum is in tetrahedral coordination [16,23]. This is in agreement with the fact that the more stable structures in basic aqueous solutions are MoO_4^{2-} and $Mo_2O_7^{2-}$ [13]. This would explain the formation of compounds of the $Na_2Mo_2O_7$ type in $Mo,Na/SiO_2$, in which 50% of Mo is placed in tetrahedral holes.

3.3. TDPAC characterization of $Mo(5\%)/SiO_2$ and $Mo(5\%),Na/SiO_2$

For the Mo/SiO_2 and $Mo,Na/SiO_2$ catalysts, it is possible to obtain a good fit of the TDPAC spectra by considering three well-defined hyperfine interactions. The TDPAC spectra and the values of the corresponding parameters are shown in figure 3 and table 3, respectively.

For the case of Mo/SiO_2, the null A signal corresponds to a null EFG in Mo-sites, thus, the related Mo-species present an environment with high symmetry. The relative concentration of these species in the $Mo(5\%)/SiO_2$ is 26%. The non-null B and C interactions are clearly distinguishable from one another fundamentally through the ω_Q parameter. The B signal presents the same ω_Q and η hyperfine parameters as Mo in an environment similar to that in MoO_3 [24,25]. Finally, the C interaction would be associated to the presence of bidimensional molybdenum species [26]. The relative concentration of these species in the $Mo(5\%)/SiO_2$ sample is approximately 16%.

From the comparison of the results obtained by LRS and TDPAC, we can conclude that there is good agreement in the identification of MoO_3 and bidimensional species of the polymolybdate type. These species correspond to non-zero B and C interactions, as indicated above.

The nature of the species associated with the A signal is not clearly established from the TDPAC results. However, by microscopic LRS spectroscopy, it was determined that one of the species present in the Mo/SiO_2 catalyst is a monomer directly joined to the support. Taking into account the properties of the silica, especially the pH at PZSC, this monomer should be an irregular octahedron. A possible structure for this monomer, compatible with the results obtained by LRS (bond-lengths) and TDPAC (zero EFG), is shown in figure 4. The values of the bond lengths and bond orders were obtained by simultaneously applying the FLS

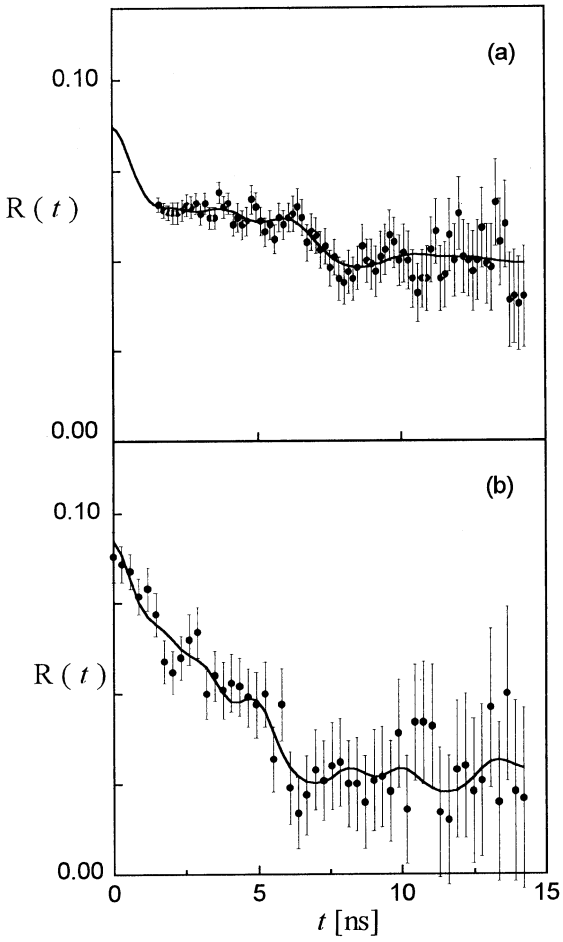

Figure 3. Typical TDPAC spectrum of ^{99}Mo measured at 650°C at air. Solid line indicates the best minimum square fit to the data compatible with three hyperfine interactions. (a) $Mo(5\%)/SiO_2$ sample, (b) $Mo(5\%),Na/SiO_2$ sample.

approximation [21] and a point-charge distribution model [27]. The point-charge distribution was calculated considering an empirical model for the bond strength vs. bond length relationship in Mo–O compounds [19]. The calculation process was carried out so as to reproduce the hyperfine parameters obtained by TDPAC for the A signal (table 3) and the Raman shift of 995 cm^{-1} corre-

Table 3
Parameters[a] of the least-square fits of the data with three hyperfine interactions for ^{99}Mo in Mo/SiO_2 and $Mo,Na/SiO_2$ catalysts

Sample	Signal	f (%)	ω_Q (Mrad/s)	η
Mo/SiO_2	A	26 (3)	null	null
	B	58 (13)	29 (3)	0.45[b]
	C	16 (3)	206 (8)	0.3 (1)
$Mo,Na/SiO_2$	A′	55 (3)	null	null
	B′	22 (3)	24 (3)	0.45[b]
	C′	23 (3)	164 (5)	0.3 (1)

[a] ω_Q and η are the hyperfine parameters that defined the electric field gradient tensor and the f parameter represents the relative population of the species associated with the corresponding signal.
[b] Fixed parameter in the fit.

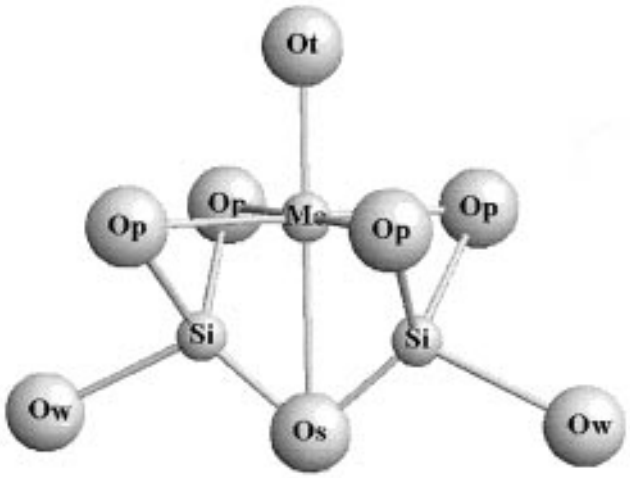

Figure 4. Proposed structure for octahedral monomers formed on Mo/SiO_2. Ot: terminal oxygen; Op: belonging to Mo–O–Si bond and located in the molybdenum plane; Os: belonging to Mo–O–Si bond; Ow: belonging to Si–O–Si bond.

sponding to the Mo=O terminal bond. A similar structure has been suggested for this monomer by Boer et al. [19] in an EXAFS-LRS study performed on Mo/SiO_2 catalysts with low molybdenum loading.

For the case of the $Mo(5\%),Na/SiO_2$ solid, a null A′ signal and two non-null B′ and C′ interactions were obtained, as in the Mo/SiO_2 case. However, for the same molybdenum loading, the Mo-site in higher concentration is now the one corresponding to the zero A′ interaction. This type of Mo-site has a contribution of 55% and should be associated with a species containing molybdenum in a highly symmetrical environment. The B′ signal presents hyperfine parameters similar to those obtained for the B signal. Instead, the hyperfine parameters of C and C′ signals are significantly different, which makes it possible to attribute a different origin to the two signals.

The LRS data may help to better assign these signals. The absence of the bands at 995 and 820 cm^{-1} in the microscopic LRS spectra of the $Mo,Na/SiO_2$ sample indicates that there is practically no bulk MoO_3. Furthermore, the LRS spectra reveal the presence of bulk species with a crystalline structure of the $Na_2Mo_2O_7$ type.

The $Na_2Mo_2O_7$ compound has two inequivalent and equipopulated crystallographical sites for Mo atoms. One of the Mo sites is octahedrally surrounded by oxygen atoms while the other is tetrahedrally coordinated. Predictions of the point-charge model, considering a charge distribution compatible with an empirical model that relates the bond length and bond strength for Mo–O and Na–O bonds [28,29], indicate that the EFG values in both Mo-sites in $Na_2Mo_2O_7$ could be responsible for the B′ and C′ TDPAC signals. The ω_Q value predicted for the octahedral Mo-site in $Na_2Mo_2O_7$ is very close to the one calculated for the octahedral Mo-site in MoO_3 while the tetrahedral one is several times higher than the octahedral site (compare signals C′ and B′ in table 3). Therefore, it can be inferred that the ^{99}Mo atoms located in the octahedral Mo-site in $Na_2Mo_2O_7$ would be responsible for the B′ signal observed by TDPAC, while the tetrahedral Mo-site in $Na_2Mo_2O_7$ would be responsible for the C′ signal.

The fact that the values of fitted parameters in the TDPAC spectrum are similar for the population of Mo-atoms responsible of signals B′ and C′ (22 and 23%, respectively) are compatible with all these atoms pertaining to the $Na_2Mo_2O_7$. In effect, as was mentioned above, the $Na_2Mo_2O_7$ have two inequivalent and equipopulated crystallographic Mo-sites. Then, this species represents approximately 45% of the Mo-species formed in the $Mo(5\%),Na/SiO_2$ catalyst. It is important to point out that there exists a good agreement between this value and the one obtained by considering that all the sodium load is forming the $Na_2Mo_2O_7$ structure.

From the results obtained by TDPAC it follows that there exist at least two species over the surface of silica modified with sodium. Signals B′ and C′ are the contribution of $Na_2Mo_2O_7$-like species, while signal A′ could be due to the presence of tetrahedral monomers directly linked to the support. Tetrahedral monomers have been detected by LRS [23,30,31] and TDPAC [15] for the case when alumina, with a pH at the PZSC of 8, was used as support. These species presented broad bands between 915 and 940 cm^{-1} and at 320 cm^{-1} [23]. In a previous work, Bañares et al. [5] reported the formation of $Na_2Mo_2O_7$ clusters, attributed to a sodium nucleation phenomenon, but they said nothing about the existence of tetrahedral monomers, the major species on our Na-modified silica surface.

LRS does not clearly indicate the existence of other species besides that of the $Na_2Mo_2O_7$ type, except for the presence of a halo with a maximum at approximately 930–950 cm^{-1}, upon which all the sharp peaks are mounted at 955, 926, 879 and 838 cm^{-1}. It is possible that the halo corresponds to the contribution of these tetrahedral monomers to the Raman signal.

The reason for the Raman signal corresponding to these tetrahedral monomers being lower than that of the $Na_2Mo_2O_7$-type (even though the former are in a higher concentration according to the TDPAC results) may be attributed to a much higher sensitivity of the crystalline species. According to the FLS approximation, these monomers would have Mo–O bond lengths and orders of 1.71–1.73 Å and 1.65–1.75 u.v. respectively. Thus, these tetrahedral monomers have a molybdic character considerably lower than the octahedral monomers and the MoO_3 present in the Mo/SiO_2 catalyst. Figure 5 shows a possible structure for these monomers which has been obtained with the FLS approximation [21] and a point-charge distribution model [27].

In brief, at least two types of species are present on the surface of silica modified by sodium: (a) crystalline

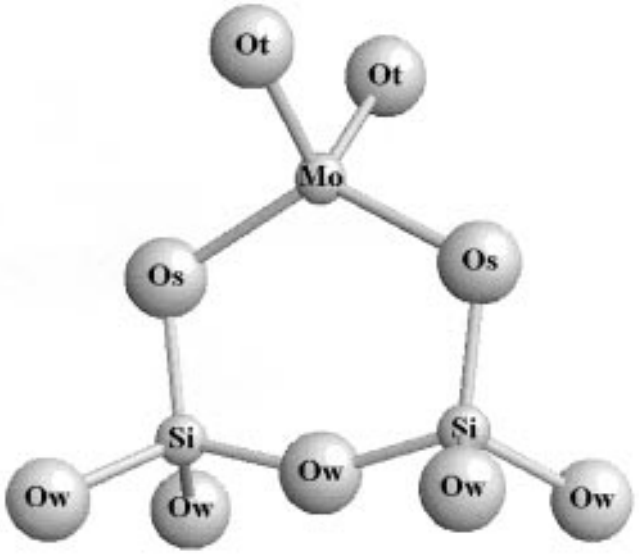

Figure 5. Proposed structure for tetrahedral monomers formed on $Mo,Na/SiO_2$. Ot: terminal oxygen; Op: belonging to Mo–O–Si bond and located in the molybdenum plane; Os: belonging to Mo–O–Si bond; Ow: belonging to Si–O–Si bond.

$Na_2Mo_2O_7$-type species; (b) tetrahedral monomers with a high degree of symmetry, directly joined to the support through two silica atoms. Signal C′, in the TDPAC characterization, might also be assigned to distorted tetrahedral monomers with non-zero EFG directly joined to the support through a single silica atom. This species gives the same EFG obtained for C′. The terminal oxygens of these monomers should interact with the surface OH groups generated by the modification of the silica surface with NaOH to equilibrate the charge balance. However, the good mass balance obtained considering that all the Na is combined as sodium molybdate would indicate that the concentration of this species would be very low.

3.4. The role of surface species in the selective oxidation of methane

Figure 6 shows catalytic data for all the catalysts reported in table 1. Increasing the molybdenum content from 1.6 to 5 wt% results in a higher conversion of methane and a lower selectivitiy to formaldehyde. The formaldehyde yield, however, increases for the higher Mo loading, which is in agreement with results reported by Suzuki et al. [11]. Upon Na addition, both conversion and selectivity decreases. This effect can be related with the results obtained by LRS and TDPAC which show that the addition of sodium to the support produces a modification in the species present on the surface. The molybdic character of the species present in the $Mo(5\%),Na/SiO_2$ solid is noticeably lower than in the $Mo(5\%)/SiO_2$, which allowed us to corroborate that the Mo=O sites play a fundamental role in this reaction as suggested by Smith and Ozkan in the case of MoO_3 crys-

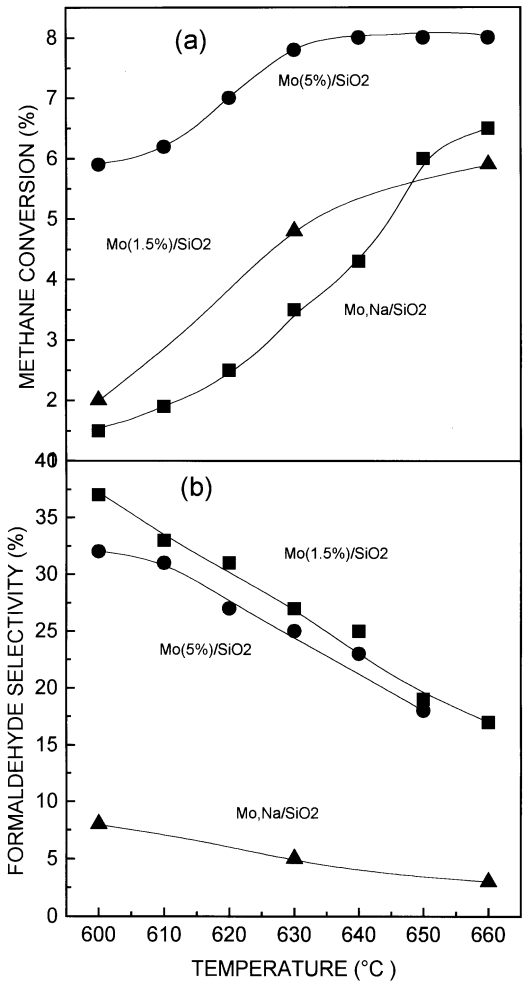

Figure 6. Catalytic behavior of Mo/SiO_2 and $Mo,Na/SiO_2$. (a) Methane conversion, (b) formaldehyde selectivity. Reaction conditions: 0.2 g of catalyst, total flow rate 17 cm^3/min, $CH_4 : O_2 = 9 : 1$.

tals [12]. A similar conclusion was reported by Irusta et al. [9,10] in the case of catalysts containing vanadium where the concentration of V=O sites was correlated with the activity of these solids.

Bañares et al. [5], employing catalysts of low molybdenum content, suggested that the activity for the reaction under study is due to the presence of monomers on the silica surface. The addition of Na notably decreases the concentration of these monomers, promoting cluster formation and, consequently, a lowering Mo dispersion. Since these monomers have a high molybdic character, the former authors' conclusion is in agreement with what we are reporting in the present work using a higher Mo loading.

However, we found out that Mo/SiO_2 and $Mo,Na/SiO_2$ catalysts with similar Mo dispersion show very different catalytic activity (see figure 6 and table 1). Both Mo/SiO_2 and $Mo,Na/SiO_2$ catalysts have clusters on the surface. MoO_3 clusters present in the former are active and selective for the reaction under study while $Mo_2Na_2O_7$ present in the latter are rather inactive. In

fact, in our case, the molybdic character is present not only in the monomeric species but also in the MoO_3 crystals present on the silica surface. These species, in which molybdenum is found in an octahedral environment, have monoxo Mo=O terminal bonds that give them a high molybdic character. The pH modification in the PZSC of the silica surface by doping with NaOH, leads to the formation of species with low molybdic character in which molybdenum is in tetrahedral coordination, such as in one of the two Mo sites in $Na_2Mo_2O_7$ and in tetrahedral monomers. These species resulted less active and selective in the oxidation of methane to formaldehyde, carbon monoxide being now the main product.

The TPR profiles show that some of the species formed on the silica surface doped with sodium are more reducible at lower temperatures than those formed on non-doped silica. This could be related to the fact that it may be easier to abstract oxygen from the Mo–O bonds of some of the tetrahedral species, probably the monomers with two terminal Mo–O bonds. This greater facility of oxygen abstraction would lead to an overoxidation of methane to carbon monoxide.

4. Conclusions

It was shown that the combined use of LRS and TDPAC resulted in a powerful tool for the identification of the molybdenum species present on the surface of a silica support. While LRS yields direct information on the nature of the species formed, and about the bond lengths and orders of these species, TDPAC gives direct information about the site structure. Moreover, TDPAC experiments are a powerful aid to quantify the molybdenum species concentration identified by these techniques.

Three main species were detected in $Mo(5\%)/SiO_2$: monomers with a single Mo=O terminal bond, small MoO_3 crystals, and polymolybdate-type species. Their proportions have been determined by TDPAC and are shown in table 3. In catalysts with a low Mo content, monomers are the main species while MoO_3 crystallites would prevail at high loadings.

The addition of sodium to the support notably decreases the molybdic character of the surface species and, consequently, conversion and selectivity are negatively affected in the oxidation of methane to formaldehyde. At least two species have been detected and characterized in the sodium-containing catalysts: crystalline $Na_2Mo_2O_7$-type species and tetrahedral monomers with a high degree of symmetry, directly joined to the support through one or two silica atoms.

Acknowledgement

Financial support was provided by CONICET PID-BID 208/92. We thank JICA (Japan International Cooperation Agency) for the donation of the ESCA-Shimadzu 750 spectrometer and the laser Raman spectrometer JASCO TRS-600SZ-P. We also thank Elsa Grimaldi for her help with the English manuscript.

References

[1] A. Bielanski and J. Haber, Catal. Rev. Sci. Eng. 19 (1979) 1.
[2] M.M. Koranne, J.G. Goodwin Jr. and G. Marcelin, J. Catal. 148 (1994) 369.
[3] N.D. Spencer, J. Catal. 109 (1988) 187.
[4] N.D. Spencer, C.J. Pereira and R.K. Grasselli, J. Catal. 126 (1990) 546.
[5] M.A.Bañares, N.D. Spencer, M.D. Jones and I.E. Wachs, J. Catal. 146 (1994) 204.
[6] M.A. Bañares and J.L.G. Fierro, in: *Catalytic Selective Oxidation*, ACS Symposium Series 523, eds. S.T. Oyama and J.W. Hightower (Am. Chem. Soc., Washington DC, 1993) p. 354.
[7] M.M. Koranne, J.G. Goodwin Jr. and G. Marcelin, J. Phys. Chem. 97 (1993) 673.
[8] B. Kartheuser and B.K. Hodnett, J. Chem. Soc. Chem. Commun. (1993) 1093.
[9] S. Irusta, A.J. Marchi, E.A. Lombardo and E.E. Miró, Catal. Lett. 40 (1996) 9.
[10] S. Irusta, L. Cornaglia, E.E. Miró and E.A. Lombardo, J. Catal. 156 (1995) 167.
[11] K. Suzuki, T. Hayakawa, M. Shimizu and K. Takehira, Catal. Lett. 30 (1995) 167.
[12] M. Smith and U. Ozkan, J. Catal. 142 (1993) 226.
[13] C.C. Willams, J.G. Ekerdt, J.M. Jengh, F.D. Hardcastle, A.M. Turek and I.E. Wachs, J. Phys. Chem. 95 (1991) 8781.
[14] D.S. Kim, K. Segawa, T. Soeya and I.E. Wachs, J. Catal. 136 (1992) 539.
[15] T. Butz, C. Vogdt, A. Lerf and H. Knözinger, J. Catal. 116 (1989) 31.
[16] H. Frauenfelder and R.M. Steffen, in: *Alpha-, Beta-, Gamma-Ray-Spectroscopy*, Vol. 2, ed. K. Siegbahn (North-Holland, Amsterdam, 1965) p. 917.
[17] M. del Arco, S.R.G. Carrazán, C. Martín, V. Rives, J.V. García-Ramos and P. Carmona, Spectrochim. Acta 50A (1994) 2215.
[18] M.A. Vuurman and I.E. Wachs, J. Phys. Chem. 96 (1992) 5008.
[19] M. de Boer, A.J. van Dillen, D.C. Koningsberger, J.W. Geus, M.A. Vuurman and I.E. Wachs, Catal. Lett. 11 (1991) 227.
[20] N. Nakamoto, *Infrared and Raman Spectroscopy of Inorganic and Coordination Compounds* (Wiley, New York, 1978).
[21] I.E. Wachs, Catal. Today 27 (1996) 437.
[22] V.H.J. Becker, Z. Anorg. Allg. Chem. 474 (1981) 63.
[23] C.C. Williams, J.G. Ekerdt, J.-M. Jehng, F.D. Hardcastle and I.E. Wachs, J. Phys. Chem. 95 (1991) 8791.
[24] C. Vogdt, T. Butz, A. Lerf and H. Knözinger, J. Catal. 116 (1989) 31.
[25] F.G. Requejo, A.G. Bibiloni, H. Saitovitch and P.R.J. Silva, Phys. Stat. Sol. (a) 120 (1990) 105.
[26] F.G. Requejo and A.G. Bibiloni, Langmuir 12 (1996) 51.
[27] A. Ralston and H.S. Wilf, eds., *Mathematical Methods for Digital Computers* (Wiley, New York, 1962) ch. 7.
[28] F.A. Schröder, Acta Cryst. B 31 (1975) 2294.
[29] I.D. Brown and R.D. Shannon, Acta. Cryst. A 29 (1973) 266.
[30] E. Payen, J. Grimblot and J. Kasztelan, J. Phys. Chem. 91 (1987) 6642.
[31] Y. Okamoto and T. Imanaka, J. Phys. Chem. 92 (1988) 7102.